nature immunology

SUPPLEMENTARY INFORMATION

https://doi.org/10.1038/s41590-020-0602-z

In the format provided by the authors and unedited.

Distinct microbial and immune niches of the human colon

Kylie R. James[1]✉, Tomas Gomes[1], Rasa Elmentaite[1], Nitin Kumar[1], Emily L. Gulliver[2], Hamish W. King[3], Mark D. Stares[1], Bethany R. Bareham[4], John R. Ferdinand[5], Velislava N. Petrova[1], Krzysztof Polański[1], Samuel C. Forster[1,2,6], Lorna B. Jarvis[7], Ondrej Suchanek[5], Sarah Howlett[7], Louisa K. James[3], Joanne L. Jones[7,8], Kerstin B. Meyer[1], Menna R. Clatworthy[1,5], Kourosh Saeb-Parsy[4], Trevor D. Lawley[1] and Sarah A. Teichmann[1,9,10]✉

[1]Wellcome Sanger Institute, Wellcome Genome Campus, Hinxton, UK. [2]Department of Molecular and Translational Sciences, Monash University, Clayton, Victoria, Australia. [3]Centre for Immunobiology, Blizard Institute, Queen Mary University of London, London, UK. [4]Department of Surgery, University of Cambridge and NIHR Cambridge Biomedical Research Centre, Cambridge, UK. [5]Molecular Immunity Unit, Department of Medicine, University of Cambridge, MRC Laboratory of Molecular Biology, Cambridge, UK. [6]Centre for Innate Immunity and Infectious Diseases, Hudson Institute of Medical Research, Clayton, Victoria, Australia. [7]Department of Haematology, Clifford Allbutt Building, Cambridge, UK. [8]Cambridge University Hospitals NHS Foundation Trust, Cambridge, UK. [9]Theory of Condensed Matter, Cavendish Laboratory, Department of Physics, University of Cambridge, Cambridge, UK. [10]European Molecular Biology Laboratory, European Bioinformatics Institute, Wellcome Trust Genome Campus, Hinxton, UK. ✉e-mail: kj7@sanger.ac.uk; st9@sanger.ac.uk

Supplementary Figure 1

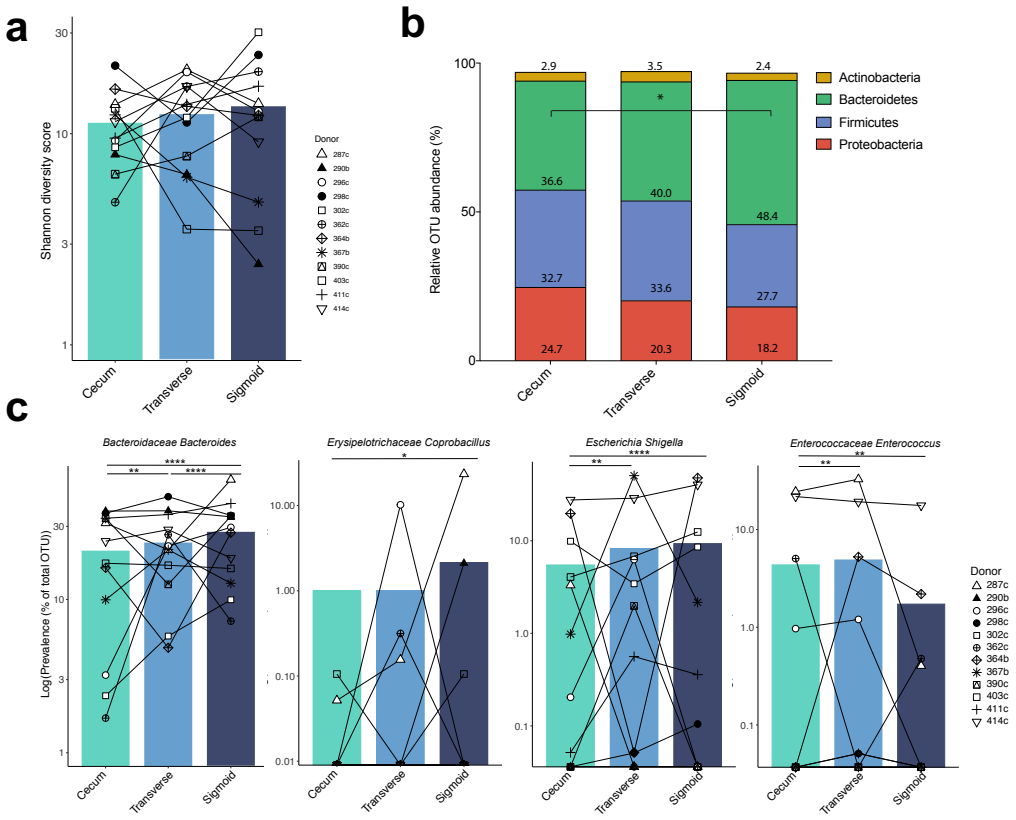

Supplementary Figure 1: Defining spatial differences in the colonic microbiome. a) Shannon diversity score of bacterial OTUs from mucosa surfaces of the cecum, transverse colon and sigmoid colon (n=12 donors). b) Relative abundances of OTUs at phylum level as in (a) with actual percentage of each phyla included. c) Relative abundances of *Bacteroides*, *Coprobacillus*, *Shigella* and *Enterococcus spp*. in colon regions as in (a), with lines connecting samples from each donor. b & c) Bars show mean proportion in each region and statistical significances are calculated from two-tailed 2-way ANOVA with Tukey's multiple corrections of the total OTU dataset. * P <0.05; ** P <0.01; **** P <0.0001

Supplementary Figure 2

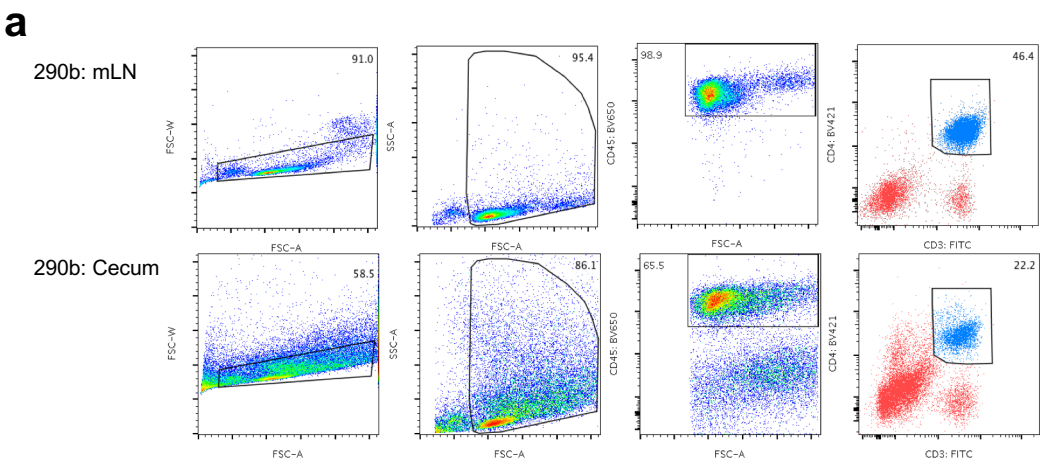

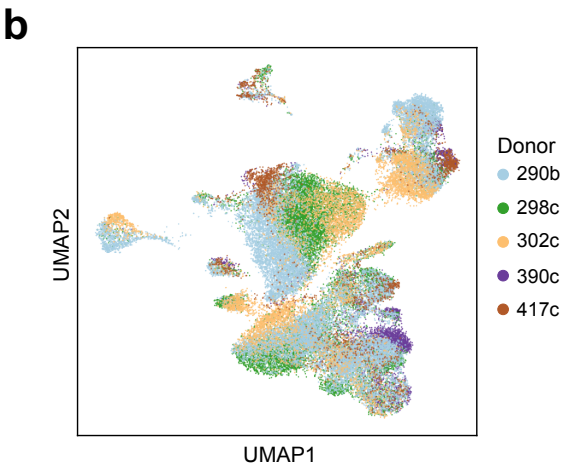

Supplementary Figure 2: Single-cell mapping of immune cells in the steady-state human colon.
a) Flow-sorting strategy for single, live, CD45$^+$, CD3$^-$, CD4$^-$ immune cells (red) and single, live, CD45$^+$, CD3$^+$, CD4$^+$ T cells (blue) from mLN (top) and colon lamina propria (bottom). b) UMAP projection of all immune cells after filtering and QC (as in Figure 2), with the five donors represented as different colours.

Supplementary Figure 3

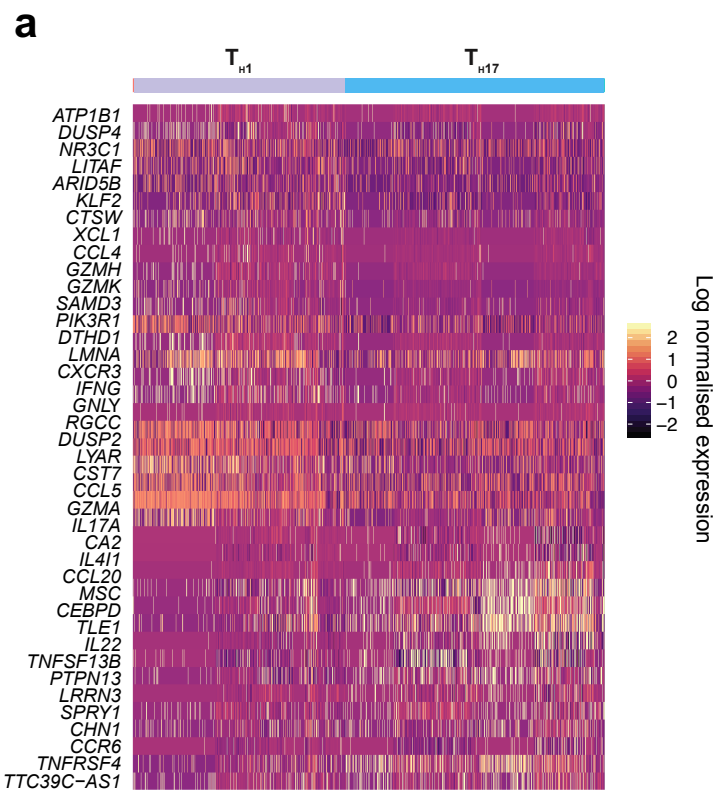

Supplementary Figure 3: Defining T helper cell transcriptional signatures in the colon. a) Heatmap of differentially expressed genes with filtering of 0.25 log fold change and minimum percent expression of 10% between T_H1 and T_H17 cells pooled from cecum, transverse colon and sigmoid colon (n=5 donors). Rows are ordered by hierarchical clustering and columns are grouped by cell type as denoted in the column annotation.

Supplementary Figure 4

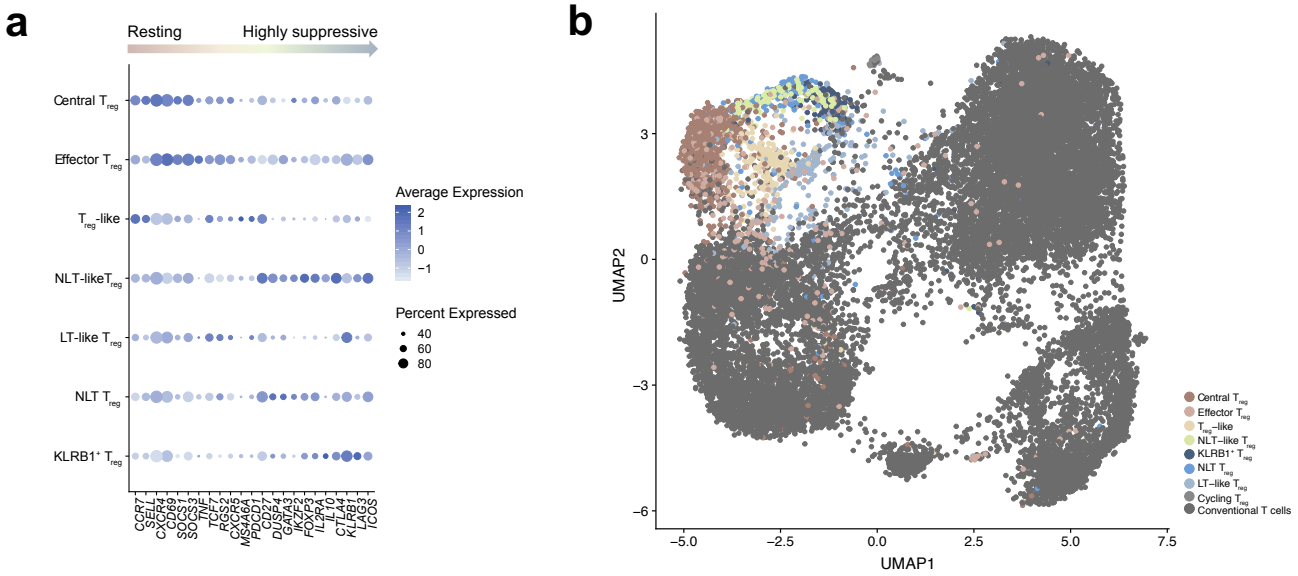

Supplementary Figure 4: T_{reg} subsets form a lymphoid-to-periphery activation trajectory.

a) Log mean expression level of marker genes used to annotate T_{reg} subsets in mLN and colon (n=5 donors). Point size shows the fraction of cells with nonzero expression. Gradient bar represents shift in cell phenotype as determined by marker gene expression. b) UMAP illustration of clustering of T_{reg} subsets and conventional CD4+ T cells of mLN and colon as in (a).

Supplementary Figure 5

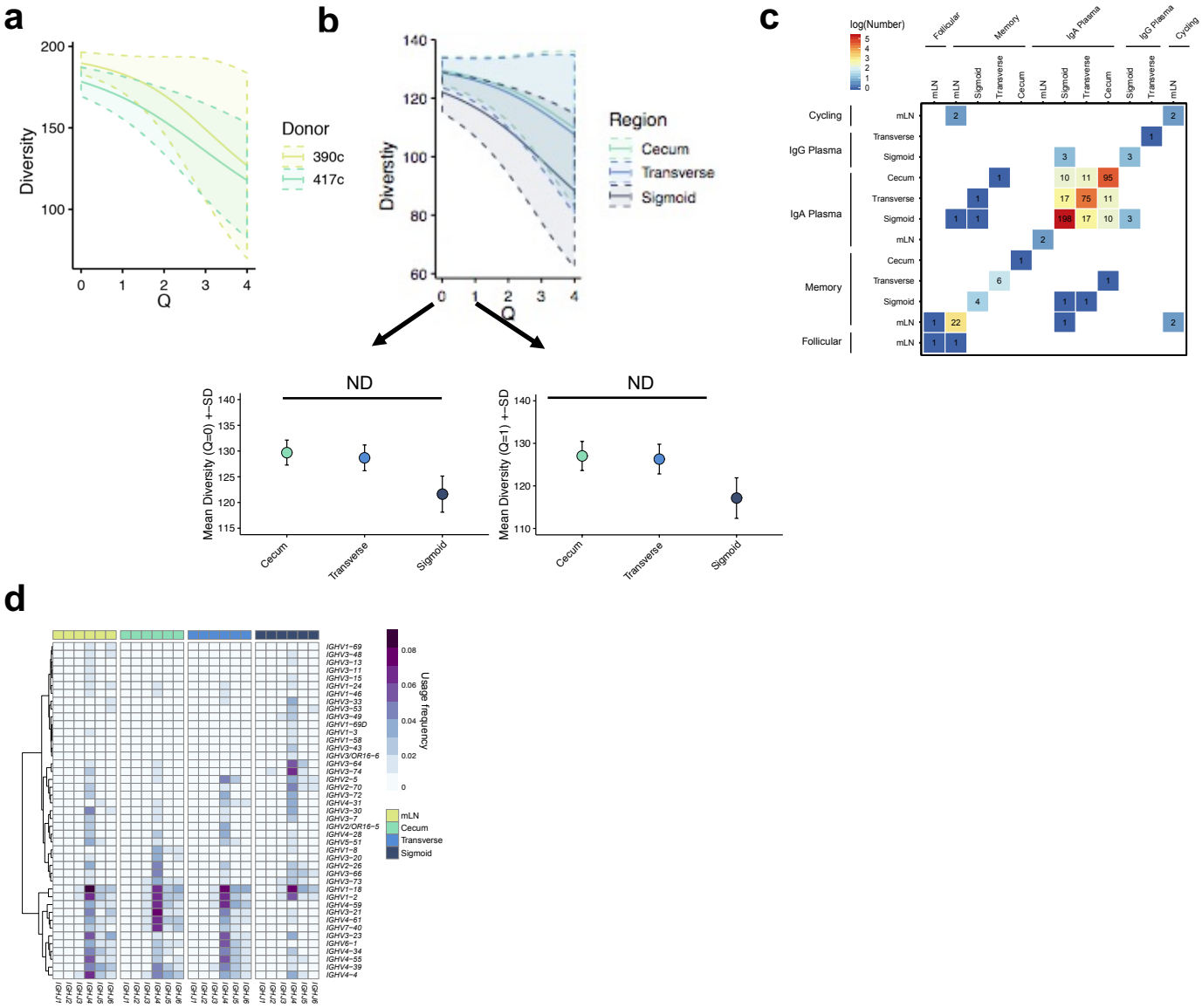

Supplementary Figure 5: Characterising B cell phenotypes and BCR expression in mLN and colon regions.

a) BCR diversity rarefaction analysis of IgA+ plasma cell clones between two donors across multiple diversity orders (Q) using single-cell VDJ-derived IgH sequences. The two groups were sampled to the number of cells of the smallest group for 500 bootstraps (n=202 per donor). The shaded area represents the 95% confidence interval. b) Expanded IgA+ plasma cell clones from both donors as in (a) were pooled and separated by gut regions. Groups were sampled to the number of cells of the smallest group (n=135 per gut region) for 500 bootstraps for BCR diversity rarefaction analysis (upper panel). The shaded area represents the 95% confidence interval for the bootstraps. Lower panels represent the results from significance tests of the diversity index between gut regions as in the upper panel at either Q = 0 (left; corresponding to species richness measure) or Q = 1 (right; corresponding to the exponential of the Shannon-Weiner index). Error bars denote standard deviation. c) Co-occurrence of expanded B cell clones identified by single-cell VDJ analysis as in (a) that are shared across different gut regions and between different cell types. Numbers reflect a binary detection event rather than the number of members per clone shared. d) Frequency of variable and joining BCR sequence expression in mLN and colon regions, detected by bulk BCR sequencing (n=3 donors). Rows are ordered by hierarchical clustering.

Supplementary Figure 6

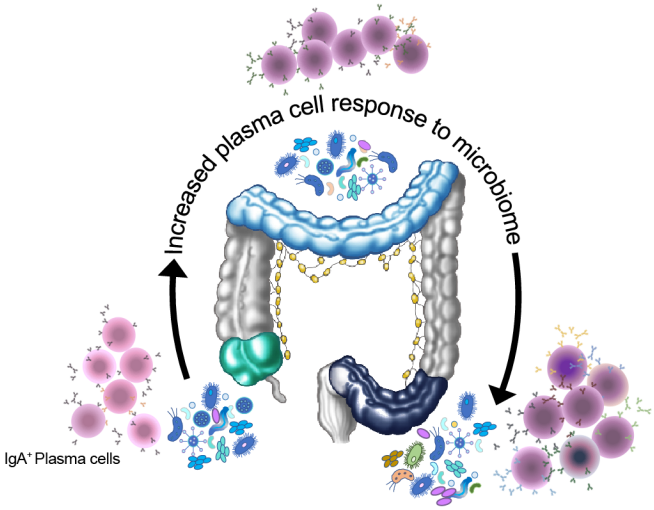

Supplementary Figure 6: Summary schematic.
Summary schematic of proximal-to-distal colon increase in accumulation, targeted migration, clonal expansion and mutation frequency of IgA^+ plasma cells, and associated increasing diversity of reactive bacteria.